IEICE The Institute of Electronics, Information and Communication Engineers

IEICE Proceeding Series

A Nonlinear Circuit Network Toward Brain Voxel Modeling

Takashi Matsubara, Hiroyuki Torikai, Tetuya Shimokawa, Kenji Leibnitz, Ferdinand Peper

Vol. 2 pp. 421-424
Publication Date: 2014/03/18
Online ISSN: 2188-5079

Downloaded from www.proceeding.ieice.org

©The Institute of Electronics, Information and Communication Engineers

2013 International Symposium on Nonlinear Theory and its Applications
NOLTA2013, Santa Fe, USA, September 8-11, 2013

A Nonlinear Circuit Network Toward Brain Voxel Modeling

Takashi Matsubara†, Hiroyuki Torikai‡,
Tetuya Shimokawa*, Kenji Leibnitz*, and Ferdinand Peper*

†Graduate School of Engineering Science, Osaka University,
1-3 Machikaneyama-cho, Toyonaka-shi, Osaka 560-8531, Japan.
‡Faculty of Computer Science and Engineering, Kyoto Sangyo University,
Motoyama, Kamigamo, Kita-ku, Kyoto-shi, Kyoto 603-8555, Japan.
* Center for Information and Neural Networks (CiNet),
National Institute of Information and Communications Technology, and Osaka University,
1-4 Yamadaoka, Suita, Osaka 565-0871, Japan.
E-mails: matubara@hopf.sys.es.osaka-u.ac.jp, torikai@cse.kyoto-su.ac.jp,
shimokawa@nict.go.jp, leibnitz@nict.go.jp, and peper@nict.go.jp.

Abstract—This paper presents a nonlinear dynamical model for predicting activities of voxels in a human primary visual cortex (V1); the activities are represented by blood-oxygen-level-dependent (BOLD) signals. The prediction performance is shown to be better than those of other traditional major models, e.g., general linear model and multivariable autoregressive model.

1. Introduction

Responses and interactions of human brain regions have been investigated from various viewpoints. Investigations of the responses and the interactions of the brain regions contribute the more accurate mapping of the network topology and the elucidation of the brain functions. The retinotopic organization is mapping of visual inputs from the retina to responded brain regions; the visual inputs are often flickering checkerboard stimuli with different polar angles and eccentricities [1–5]. The responses of the brain regions are sampled by using functional magnetic resonance imaging (fMRI), which detects the blood-oxygen-level-dependent (BOLD) signals; the scanned spatial unit is called "voxel". Traditionally, the responded voxels have been identified by using cross correlation [2] and covariance [3,4] between the visual inputs and the BOLD signals. In addition, the BOLD signals are predicted by general linear model (GLM) [5,6]; this is on the assumption that the BOLD signals are calculated by summation of the visual inputs and do not have any dynamics. On the other hand, the brain voxel dynamics and their interactions represented by BOLD signals are often modeled in a little more complicated ways: multivariable autoregressive model (MARM) [7–9] and dynamic causal model (DCM) [10,11]. The linear and bilinear models are simple and versatile models, but not specifically designed for the brain voxel dynamics. More appropriate and powerful model is needed. This paper focuses on the dynamic responses of voxels in the human primary visual cortex (V1) to the visual inputs and models them in a more sophisticated way.

2. Integrate and Oscillate Model

This section models the dynamic responses of voxels in the human primary visual cortex (V1) to the visual inputs; the model is called "integrate and oscillate model" (IOM) hereafter. The visual inputs consist of some types of flickering checkerboard stimuli, which are indexed by $i \in \mathbf{I} \equiv \{0, 1, \dots\}$. For simplicity, the interactions between voxels are ignored and the voxel dynamics are assumed to be affected only by the visual inputs. A BOLD signal is scanned with a period of T, and the n-th scanned BOLD signal of a voxel is expressed as $x(n) \in \mathbf{R}$ $(n = 0, 1, \dots)$. A predicted value of the n-th scanned BOLD signal $x(n)$ is denoted by $y(n)$ hereafter. In addition, each visual input i is expressed as

$$I_i(n) = \begin{cases} 1 & \text{if the visual input } i \text{ is} \\ & \text{applied at the time } n, \\ 0 & \text{otherwise}. \end{cases}$$

This paper presents the IOM described by the following equation:

$$y(n) = v(n) + A(n)\cos(\theta(n)) + k.$$

$v(n)$ is a major component, $A(n)$ and $\theta(n)$ are an amplitude and an angle of a minor component, respectively, and the dynamics of which are described by

$$\begin{aligned} v(n+1) &= v(n) + b\left(\textstyle\sum_{i\in\mathbf{I}} a_i I_i(n+1) - v(n)\right), \\ \theta(n+1) &= \theta(n) + \omega + \omega^{\mathrm{v}} v(n), \\ A(n+1) &= A_0 + A^{\mathrm{v}} v(n+1), \end{aligned} \tag{1}$$

where the DC bias k, the coefficients b, a_i $(i \in \mathbf{I})$, the angular velocity coefficient w^{v}, the basic radius

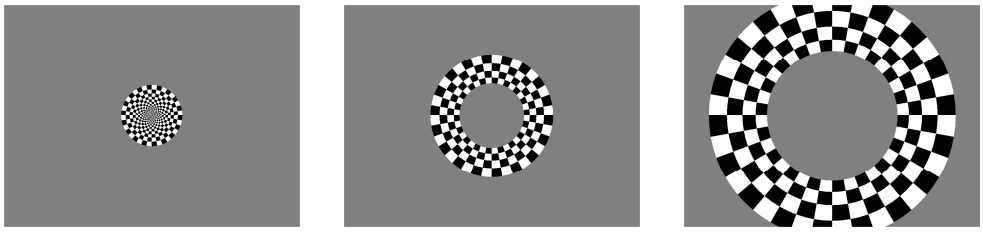

visual input $i = 0$ visual input $i = 1$ visual input $i = 2$

Figure 1: The three types of flickering checkerboard stimuli.

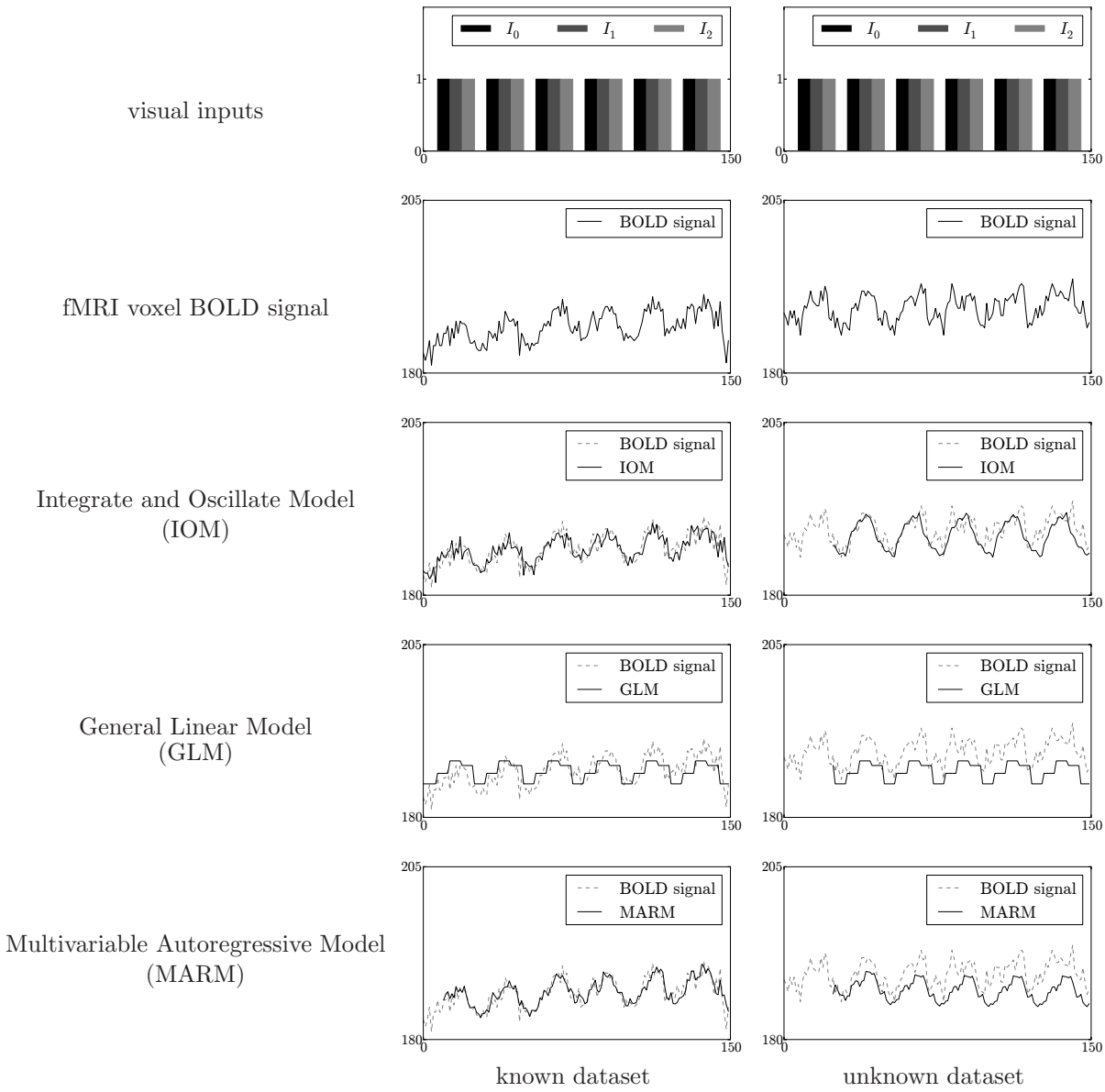

Figure 2: The visual inputs, the BOLD signal $x(n)$ of a V1 voxel, and the predicted BOLD signals $y(n)$of the IOM, the GLM, and the MARM, from top to bottom. Each left (right) figure shows the known dataset (the unknown dataset).

A_0, and the radius coefficient A^{v} are parameters. In dynamical system viewpoint, v is a slow major stimulus-induced dynamics and θ is a fast minor semi-autonomous dynamics.

fMRI Scan Dataset and Parameter Fitting: The scan dataset is sampled with the conditions as provided below. The visual inputs are 375 second time length and consist of the three types of flickering checkerboard stimuli shown in Fig. 1, which are indexed by $i \in \mathbf{I} \equiv \{0, 1, 2\}$ from left to right. The BOLD signals $x(n)$ are scanned by 3 T MRI (3 mm thick) and the scan period is $T = 2.5$[sec], and thus, each recorded time series $x(n)$ contains 150 scans. The MNI coordinate of the scan dataset is transformed to the Talairach coordinate [12, 13] and each voxel is labeled by the Talairach client [13–15]. The visual inputs and an example of the BOLD signal of a V1 voxel are shown in the upper left figures in Fig. 2.

The parameters k, b, a_i ($i \in \mathbf{I}$), w^{v}, A_0, and A^{v}, and the initial states $v(0)$ and $\theta(0)$ of the IOM are initialized randomly and updated by a simple 2-opt search algorithm for minimizing the root-mean-square error (RMS). The center left figure in Fig. 2 also shows the predicted BOLD signal $y(n)$ of the IOM after parameter fitting.

Other Traditional Modelings: General linear model (GLM) is expressed as the following equation:

$$y(n) = \sum_{i \in \mathbf{I}} a_i I_i(n) + k,$$

where the coefficients a_i ($i \in \mathbf{I}$) and the DC bias k are parameters.

Multivariable autoregressive model (MARM) is expressed as the following equation:

$$y(n+1) = \sum_{j=0}^{p-1} \left(a_j y(n-j) + \sum_{i \in \mathbf{I}} b_{i,j} I_i(n-j) \right),$$

where the degree p of the MARM, and the coefficients a_j and $b_{i,j}$ ($i \in \mathbf{I},\ j = 0, \ldots, p-1$) are parameters. In this paper, $p = 10$ is used.

Performance Comparison: For testing the performance of predicting an unknown dataset, another scan dataset with the same conditions as above is provided; the first 24 scans are used for estimating the internal states (i.e., the initial states $v(0)$ and $\theta(0)$ and the DC bias k) and the other 126 scans are used for performance test. The prediction performance is evaluated by the average of the prediction errors (i.e., the RMS) of 50 randomly chosen V1 voxels which have high covariances ($r \geq 0.5$) with the summation $I = \sum_{i \in \mathbf{I}} I_i$ of the visual inputs. Fig. 2 shows the BOLD signal $x(n)$ of the unknown scan dataset, and the predicted BOLD signals $y(n)$ of the IOM, the GLM, and the MARM. The average RMS are summarized in Table 1, which implies that the IOM is the best way for predicting the BOLD signals of V1 voxels.

Table 1: BOLD Signal Prediction Performance

Model	**Average RMS for**	
	known dataset	**unknown dataset**
IOM	1.90	2.45
GLM	2.29	3.78
MARM	1.23	3.21

3. Conclusion

This paper has presented a novel model "integrate and oscillate model" (IOM), which predicts BOLD signals of V1 voxels responded to visual inputs. The prediction error of the IOM has been shown to be small with compared to those for the other major BOLD signal prediction models: general linear model and multivariable autoregressive model. That is, the IOM has been confirmed to be a better way for predicting BOLD signals of V1 voxels. Future work includes: (a) modeling the interactions between brain voxels, (b) a theoretical analysis of the IOM, (c) prediction performance testing on the BOLD signals responded by more complicated visual inputs, and (d) prediction performance comparison with the other major BOLD signal prediction models, e.g., DCM.

The authors would like to thank Yusuke Morito of National Institute of Information and Communications Technology for providing BOLD signal data. The authors would like to also thank Professor Toshimitsu Ushio of Osaka University for helpful discussions. This work was partially supported by the Support Center for Advanced Telecommunications Technology Research (SCAT), Grant-in-Aid for JSPS Fellows, KAKENHI (24700225), the Telecommunications Advancement Foundation (TAF), and Toyota Riken Scholar.

References

[1] R. B. Tootell *et al.*, "Functional analysis of primary visual cortex (V1) in humans." *Proceedings of the National Academy of Sciences of the United States of America*, vol. 95, no. 3, pp. 811–7, 1998.

[2] W. Chen *et al.*, "Mapping of lateral geniculate nucleus activation during visual stimulation in human brain using fMRI." *Magnetic Resonance in Medicine*, vol. 39, no. 1, pp. 89–96, 1998.

[3] K. A. Schneider, M. C. Richter, and S. Kastner, "Retinotopic organization and functional subdivisions of the human lateral geniculate nucleus: a high-resolution functional magnetic resonance imaging study." *The Journal of Neuroscience*, vol. 24, no. 41, pp. 8975–85, 2004.

[4] K. A. Schneider and S. Kastner, "Visual responses of the human superior colliculus: a high-resolution functional magnetic resonance imaging study." *Journal of Neurophysiology*, vol. 94, no. 4, pp. 2491–503, 2005.

[5] D. Bressler, N. Spotswood, and D. Whitney, "Negative BOLD fMRI response in the visual cortex carries precise stimulus-specific information." *PloS ONE*, vol. 2, no. 5, p. e410, 2007.

[6] K. Friston, A. Holmes, and J. Poline, "Analysis of fMRI time-series revisited," *NeuroImage*, vol. 2, no. 1, pp. 45—-53, 1995.

[7] R. Goebel *et al.*, "Investigating directed cortical interactions in time-resolved fMRI data using vector autoregressive modeling and Granger causality mapping," *Magnetic Resonance Imaging*, vol. 21, no. 10, pp. 1251–1261, 2003.

[8] A. Roebroeck, E. Formisano, and R. Goebel, "Mapping directed influence over the brain using Granger causality and fMRI." *NeuroImage*, vol. 25, no. 1, pp. 230–42, 2005.

[9] D. Marinazzo *et al.*, "Nonlinear connectivity by Granger causality." *NeuroImage*, vol. 58, no. 2, pp. 330–8, 2011.

[10] K. Friston, L. Harrison, and W. Penny, "Dynamic causal modelling," *NeuroImage*, vol. 19, no. 4, pp. 1273–1302, 2003.

[11] S. M. Smith *et al.*, "Network modelling methods for FMRI." *NeuroImage*, vol. 54, no. 2, pp. 875–91, 2011.

[12] J. Talairach and P. Tournoux, *Co-Planar Stereotaxic Atlas of the Human Brain: 3-D Proportional System: An Approach to Cerebral Imaging*. Thieme, 1988.

[13] J. L. Lancaster *et al.*, "Bias between MNI and Talairach coordinates analyzed using the ICBM-152 brain template." *Human Brain Mapping*, vol. 28, no. 11, pp. 1194–205, 2007.

[14] "talairach.org." url: http://www.talairach.org/

[15] J. L. Lancaster *et al.*, "Automated Talairach atlas labels for functional brain mapping." *Human Brain Mapping*, vol. 10, no. 3, pp. 120–31, 2000.